Journal of Hydrology 405 (2011) 1–9

Contents lists available at ScienceDirect

Journal of Hydrology

journal homepage: www.elsevier.com/locate/jhydrol

Three-dimensional high resolution fluvio-glacial aquifer analog: Part 1: Field study

P. Bayer [a,*], P. Huggenberger [b], P. Renard [c], A. Comunian [c]

[a] ETH Zürich, Engineering Geology, Sonneggstrasse 5, 8092 Zürich, Switzerland
[b] University of Basel, Geological Institute, Bernoullistrasse 32, 4056 Basel, Switzerland
[c] University of Neuchâtel, Centre of Hydrogeology and Geothermics (CHYN), Rue Emile-Argand 11, 2000 Neuchâtel, Switzerland

ARTICLE INFO

Article history:
Available online 1 April 2011
This manuscript was handled by P. Baveye, Editor-in-Chief

Keywords:
Aquifer analog
Unconsolidated sediment
Digital mapping
Ground penetrating radar (GPR)
Hydrofacies
Heterogeneity

SUMMARY

Describing the complex structures that exist in many sedimentary aquifers is crucial for reliable groundwater flow and transport simulation. However, hardly any aquifer can be inspected in such detail that all decimeter to meter heterogeneity is resolved. Aquifer analogs serve as surrogates to construct models of equivalent heterogeneity, and thus imitate those features relevant for flow or transport processes. Gravel pits found in excavation show excellent sections of the sedimentary sequence and thus offer direct insight into the structural and textural composition of the subsoil. This paper describes an approach to also inspect the third dimension: by mapping during the ongoing excavation it is possible to obtain a three-dimensional representation of the subsurface within a short period of time. A detailed description of a case study is presented and the findings from sedimentological, hydrogeological and geophysical analyses are compared. The gravel pit is located near the town of Herten in southwest Germany, where relatively young unconsolidated fluvio-glacial and fluvial sediments in the Rhine basin are mined. The excavated gravel body is built up by architectural elements typical for braided river deposits. The study generated a high-resolution data set of lithofacies, hydrofacies and ground penetrating radar (GPR) profiles. It represents the basis for a full three-dimensional geostatistical reconstruction presented in the second part (Comunian et al., 2011).

1. Introduction

Sedimentary aquifers in river valleys host many of the important shallow aquifers in Central Europe. Among these are late Pleistocene unconsolidated fluvio-glacial and fluvial braided river sediments in the Rhine basin. They are often built up by non-uniform sequences of layers, cross-beddings and deposits that are gradually changing. Such features can hardly be modeled by simple interpolation between point measurements or standard geostatistical methods (Anderson, 1989; Jussel et al., 1994; Weissmann and Fogg, 1999; Chen et al., 2010). Even advanced noninvasive techniques such as modern tomographical or georadar geophysical examination can only approximate subsurface structures (e.g. Becht et al., 2007; Brauchler et al., 2010) and often deliver non-unique results. Hydrogeological and geophysical site investigation thus is ideally complemented by process-based geological analysis and characterization of deposition environments. Integrating this source of "soft information" in the model building process is fundamental for building realistic conceptual geological models. However, due to the complexity of the braided river systems, there is still a lack of combinations of sedimentological, hydrogeological and geophysical analyses of different sites that portray the character and the band-with of heterogeneity scales in this type of deposits. As a consequence, it is important to develop methods to capture the essence of such a deposit with respect to heterogeneity characterization at different scales, which is a main topic of the field investigation methods presented in this study.

Sedimentological analysis and interpretation can offer a systematic framework for reconstruction of architectural elements and their spatial continuities (Scheibe and Freyberg, 1995; Fraser and Davis, 1998; Heinz et al., 2003; Ezzy et al., 2006). Utilizing this knowledge is fundamental to achieve a geologically plausible description of heterogeneity, to delineate ranges of high-conductivity zones and for consistent re-interpretation of geophysical data (Stanford and Ashley, 1998; Asprion and Aigner, 1999; Hyndman and Tronicke, 2005; Iversen et al., 2008). Inclusion of such information in hydrogeological model calibration prevents non-realistic realizations of spatial hydraulic parameter distribution and exploits complementary knowledge to reduce ill-posedness of (geostatistical) inversion problems (Chen and Rubin, 2003; Maier et al., 2009; Dafflon et al., 2010). Even in case of significant data scarcity, a conceivable portrayal of the subsurface,

* Corresponding author. Tel.: +41 44 63 36829.
E-mail addresses: bayer@erdw.ethz.ch (P. Bayer), peter.huggenberger@unibas.ch (P. Huggenberger), philippe.renard@unine.ch (P. Renard), alessandro.comunian@unine.ch (A. Comunian).

0022-1694/$ - see front matter © 2011 Elsevier B.V. All rights reserved.
doi:10.1016/j.jhydrol.2011.03.038

which would hardly be possible based on only a few measurements, is feasible.

For bringing together sedimentological and hydrogeological characterization, aquifer analog studies have become popular, particularly in the last decade: vertical outcrops of sedimentary bodies are inspected in detail to obtain a model imitate of the real reservoirs that is as exact as possible (e.g. Smith, 1989; Huggenberger and Aigner, 1999; Heinz et al., 2003; Bersezio et al., 2007, Huysmans et al. 2008). Such accuracy means a considerable workload, because sedimentary facies may vary on the centimeter scale. Facies types have to be categorized with respect to sedimentary and hydrogeological criteria. Lithofacies reflect well defined deposition events or environments, whereas hydrofacies stand for quasi-homogeneous sub-units that can be characterized by single representative hydraulic and/or hydrochemical parameters (Anderson et al., 1999; Klingbeil et al., 1999; Ouellon et al., 2008). These parameters have to be determined by appropriate field and lab methods.

A major problem is that analogs are usually obtained from single outcrop walls, which only deliver a cross-sectional profile but hardly capture the true three-dimensional conditions. The present work reports a previously unpublished comprehensive three dimensional aquifer analog study on an unconsolidated braided river deposit at the scale of tens of meters (Bayer, 2000). A gravel pit found in excavation showed excellent sections of the sedimentary sequence and thus offered direct insight into the structural and textural composition of the subsoil. Study of lithofacies and hydrofacies distribution is supplemented by ground penetrating radar (GPR) measurements that were conducted before mining.

The presented mapping enables the detailed comparison of hydrogeological, sedimentological and geophysical investigations. This inspected scale is of importance, for instance at the scale of smaller to medium scale contaminant sources of spills and proximal plumes downstream. Meanwhile, several recent studies have used part of the data set for demonstration of geophysical forward (Kowalsky et al., 2001) or inverse modeling (Hu et al., 2009), for hydraulic or transport modeling (Maier et al., 2005; Maji et al., 2006; Werth et al., 2006), and for sedimentological analysis (Heinz et al., 2003). The developed dataset is provided as downloadable supplement and may be used in realistic 3D hydrogeological modeling studies. The companion paper (Comunian et al., 2011) presents how such a data set can be used to obtain a full 3D model using classical and multiple point geostatistical techniques.

2. Architecture and facies types

2.1. Sedimentological setting and concept

The study site is located in the upper Rhine valley in Southern Germany close to the Swiss border near Basel and 500 m west of the town of Herten (see Fig. 1, Kieswerk Rheinfelden, Gauss Krueger right value 3403877, Gauss Krueger high value 5268837; 276 m a.s.l). The gravel deposits in this area originate from glacial outwash 50 km downstream of the front of the Rhine-glacier. A sediment accumulation phase at the glacier front reached its maximum 18,000 a BP (i.e., years before present) and down river, in the Basel region about 12,000 a BP (see Kock et al., 2009). Several degradation phases followed and formed series of river terraces. The sedimentary structures outcropping as nearly vertical sections in various gravel pits clearly document the braided character of the majority of the deposit. Exceptions are remnants of poorly sorted coarse gravel documenting events of high flows with an erosional episode followed by deposition of gravel. Overbank deposits are

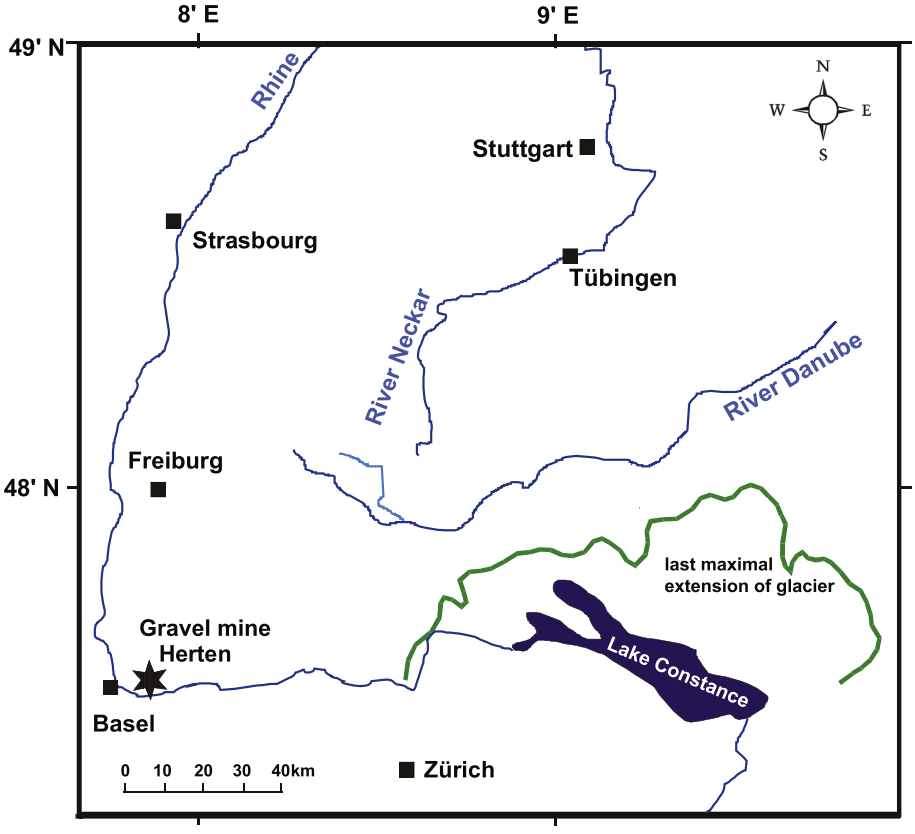

Fig. 1. Map of Herten gravel pit location in SW Germany at the SW bend of the River Rhine.

quasi absent, indicating a large lateral channel mobility of the active channel belt or a lateral extent of the active channel belt including the entire valley floor, at least for the aggrading phase.

Among others, Siegenthaler and Huggenberger (1993), Beres et al. (1995), Heinz and Aigner (2003b) and Heinz et al. (2003) intensively studied the pro-glacial environment along the river Rhine. They interpreted their observations from multiple outcrop studies with respect to depositional conditions and presented regional facies models that can be distinguished according to discharge types (main, intermediate, minor discharge area) of the former glacier outwash plain. The Herten gravel body is part of the main discharge area, including high-energetic depositions of coarse sediments. In the following, the genetic classification and sedimentological interpretation will only be tangent and the reader is referred to Heinz and Aigner (2003b) and Kostic et al. (2005) for more details.

Lithofacies and sedimentary structures of the Herten gravel body have been carefully mapped, from the maximum aggradation level, in a series of parallel outcrops, oriented in east–west direction more or less parallel to the former River Rhine. To perform a genetic analysis on such deposits, several scales need to be taken into consideration. On the small scale (decimeter), separate lithofacies types with comparable structural and textural characteristics and which stem from similar transport and depositional processes are distinguished. On the larger scale (meter), architectural elements can be differentiated according to characteristic element boundaries (generally made up of erosional surfaces and in some cases, but in the Rhine gravel rarely, of former geomorphological surfaces). These architectural elements include cut-and-fill elements and accretionary elements as well as transitional categories between these two types. The former is the result of a process in which an erosive phase creates scours. Flow separation between channel bases causes scours to be filled with well sorted open framework and bimodal gravel sediments (Heinz et al., 2003). The gouging is usually characterized by internal trough-shaped cross-beddings that can be composed of alternating sequences. Here, lithofacies varies on the decimeter-scale. These cut-and-fill elements (e.g. scour pools) are frequent in the main discharge area in the Rhine valley and also typical for the central part of the strata studied at the Herten site.

Accretionary elements (e.g. gravel sheets) are interpreted as accumulations in the active channel belt and dominate distant discharge areas. Usually, unarticulated horizontal layer units of matrix-dominated gravel grow over a continuously flat base. In contrast to the cut-and-fill elements, they appear homogeneous and can show significant lateral extension to hundreds of meters.

2.2. Lithofacies

The classification into small-dimensional sedimentological units is, for the most part, based on the classification used by Keller (1996) and Heinz and Aigner (2003b). According to this system, it is possible to differentiate between typical lithofacies types that can be characterized by the spectrum of grain sizes, the sorting, level of roundness, and the composition of the particles, as well as the structure and the layering.

A code ($[i_1]I_1i_2i_3[i_4]$) is used, which for each facies combines a unique sequence of indices that represent abbreviations for typical features. Index I_1 denotes the main grain size, and optionally i_1 may be considered to describe subordinate components or matrix. For specification of I_1, we find gravel (G) and sand (S) dominated facies types, as well a mixture of both (GS). Index i_1 highlights the appearance of cobbles (c), sand (s) or fines (f). The texture (c: clast-supported, m: matrix-supported) is indicated by the next code letter, i_2. This may be not further specified in well sorted facies and accordingly represented by i_2 = '–'. The following index i_3 reflects stratification: x: stratified, m: massive (no bedding), g: graded. Additional information may be added, separated by a comma as i_4. This includes alternation (a), open framework (o) and bimodal structure (b).

At the Herten quarry site, four lithofacies types are distinguished:

- poorly sorted gravel (*Gcm*): gravel with a broad grain size distribution, cobbles and also sand as secondary components; the layered appearance is due to changing sand content, but imbrication of particles indicates horizontal- to cross-bedding; this litho- and hydrofacies originates from bedloads of high-energetic flood events (Klingbeil et al., 1999; Heinz et al., 2003b); it can be of significant lateral extension up to hundreds of meters and as such form accretionary elements (Fig. 2a).
- alternating gravel (*Gcg, a*): sequence of matrix-filled (bimodal) and matrix-free (open framework) gravel; lower, bimodal unit with matrix and made of sand or silt; horizontal to cross-bedding; typical deposit of cut-and-fill elements, which can appear in different variants, partly eroded and incomplete (Fig. 2b).
- well sorted gravel and sand (*GS-x*): mixture of gravel and sand, matrix- or component-based; often cross-bedded, sheet-bound grain size change; interpreted as typical bedload deposit in high-energetic fluvial systems (Heinz et al., 2003b) (Fig. 2a).
- pure sand (*S-x*): very well sorted sand with occasional gravel debris, horizontal- to cross-bedding; occurs rarely at Herten site and typically represents low-energetic bedload deposit (Fig. 2c).

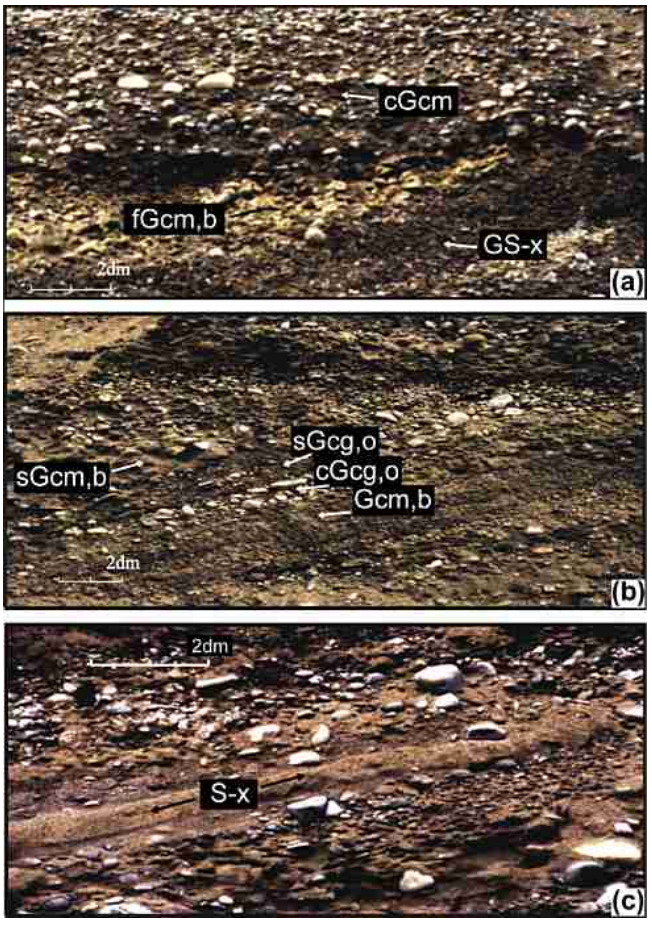

Fig. 2. Photos of typical lithofacies and hydrofacies at study site: (a) poorly and well sorted gravel, (b) alternating gravel, and (c) well sorted sand.

Table 1
Litho- and hydrofacies types at Herten site with hydraulic properties. Except of those for the hydrofacies cGcm, sGcm, b and fGcm, b, the ranges of hydraulic conductivities are taken from referenced previous studies. The range for cGcm is approximated by that measured by Heinz et al. (2003) for Gcm, for sGcm, b the range measured by Heinz et al. (2003) for sGcm is suggested. No range is available for fGcm, b, but it is expected to be about $\pm 1 \times 10^{-6}$ m/s, i.e. in the order of magnitude of the listed mean hydraulic conductivity. Porosity ranges are only listed when given in previous work.

Lithofacies code	Description	Hydro-facies code	Further description	Hydraulic conductivity K (m/s)	Porosity	References
Gcm	Poorly sorted, matrix supported gravel	Gcm	Normal	$2.5 \times 10^{-4} \pm 2.1 \times 10^{-4}$	0.17 ± 0.07	(2)
		cGcm	Cobble-rich	$2.3 \times 10^{-4} \pm 2.1 \times 10^{-4}$	0.15 ± 0.01	(2)
		sGcm	Sand-rich	$6.1 \times 10^{-5} \pm 5.9 \times 10^{-5}$	0.13 ± 0.04	(2)
Gcg,a	Alternating gravel	Gcg, o	Matrix-free, clast-supported open framework coarse–fine pebbles	$2.6 \times 10^{-2} \pm 2.3 \times 10^{-2}$	0.26 ± 0.02	(3)
		cGcg, o	Cobbles-coarse pebbles openwork	$1.3 \times 10^{-1} \pm 7.4 \times 10^{-2}$	0.26 ± 0.02	(3)
		sGcg, o	Granules/sand open framework	$9.5 \times 10^{-2} \pm 6.5 \times 10^{-3}$	0.23	(2)
		sGcm, b	Bimodal basal subunit with sand matrix	$4.3 \times 10^{-5} \pm 1.8 \times 10^{-4}$	0.22	(1), (2)
		fGcm, b	Bimodal basal subunit with silt/clay matrix	6.0×10^{-7}	0.20	(1), (2)
GS-x	Well sorted gravel (and coarse sand)	*GS-x*		$2.3 \times 10^{-3} \pm 4.5 \times 10^{-3}$	0.27 ± 0.07	(2)
S-x	Pure, well sorted sand	*S-x*		$1.4 \times 10^{-4} \pm 5.0 \times 10^{-3}$	0.36 ± 0.04	(2)

(1) Bayer, 2000, (2) Heinz et al., 2003, (3) Kostic et al., 2005.

2.3. Hydrofacies

The lithofacies classification relies on physical attributes that allow direct subdivision of outcrop walls into the sedimentary categories. Mosaics can be generated that are clustered in well-defined sub-units. Such lithofacies types are distinguished from a sedimentological perspective and cannot always be converted to hydrofacies classes. For example, for genetic reasons it is common to combine typical sequences of alternating gravel beddings (*Gcg, a*) into one lithofacies cluster. A basal matrix-supported gravel unit is overlain by sequences of clast-supported, matrix-free gravels (open framework) (Fig. 2b). The lower part shows a substantially lower hydraulic conductivity than the upper highly permeable open framework. Consequently, it is reasonable to further subdivide such lithofacies into subclasses of different hydrofacies. Vice versa, different lithofacies types with similar hydraulic properties may be combined into one single hydrofacies.

In contrast to lithofacies, hydrofacies can quantitatively be described by the specific hydraulic parameters. Thus classification based on hydrofacies means that facies with the same or comparable permeability and porosity could be merged. Heinz et al. (2003) and Kostic et al. (2005) present the results from laboratory measurements (using permeameter columns) that are complemented by empirical estimation of hydraulic conductivity based on the grain size distribution. The measurements with multiple samples show a considerable variability, in particular for the matrix-supported facies types. Therefore, former estimations presented by Huggenberger et al. (1988), Jussel et al. (1994), Kleineidam (1998), Klingbeil et al. (1999) and Bayer (2000) can differ compared with the findings from the later, more comprehensive analyses as presented by Heinz et al. (2003). Table 1 lists the specifications taken from Bayer (2000), Heinz et al. (2003), and Kostic et al. (2005), whereas the latest are considered the more realistic and precise data. Partially empirical values as given in the original work (Bayer, 2000) are replaced by later experimental conductivity and porosity estimates. In a comprehensive overview, Zappa et al. (2006) compiled the hydraulic data from different studies on alluvial sediments. Kleineidam et al. (1999) also examined the chemical properties of the sand and gravel grains collected from the braided river sediments in the Rhine valley.

As presented in Table 1, hydrofacies follow the lithofacies classification. However, the poorly sorted gravel, *Gcm*, as well as the alternating gravel, *Gcg, a*, are subdivided into separate hydrofacies types (see also Fig. 2a and b), which results in a total of ten categories. For the massive gravel, sandy and cobble-rich variants are distinguished, which can be characterized by individual conductivity and porosity values. As mentioned above, the alternating sequence can be further differentiated according to the gradation. Apparently, though considered as single sedimentological unit, the *Gcg, a* spans a wide range of hydraulic conductivity values over nearly seven orders of magnitude. Of major hydraulic importance appear the highly conductive, matrix free compartments of typically thin open framework deposits (*Gcg, o*).

The lithofacies-based sub-classification of hydrofacies types is standardized (e.g. Heinz et al., 2003), but could be simplified. For example, nearly the same conductivities are measured for sGcm, b and sGcm; also Gcm and cGcm appear to be similar. Therefore depending on the specific hydrological objectives, it appears desirable to combine those hydrofacies types listed in Table 1 into major groups. For example, an option is to cluster and visualize them based on a log scale as will be done in the remainder of this study.

2.4. GPR and radar facies

Before excavation, the sedimentary block was examined by a ground penetrating radar (GPR) survey. GPR is a fast, inexpensive and established geophysical technique for non-invasive collection of stratigraphical data (e.g. Huggenberger, 1993; Jol, 2009). It utilizes high-frequency electromagnetic waves that are sent in the ground, where they propagate (for gravels mostly in the order of 8–11 cm/ns), are refracted, reflected or attenuated. Changes in residual water content, clay fraction and grain size distribution determine the reflection coefficients of the different materials. The two-way travel-times of the returning signals are recorded. The vertical resolution of sedimentary structures is in the order of a quarter wave length, for gravel at the 10 cm scale. However, for a given wave length, resolution decreases with depth (i.e. increasing size of footprint with time, Daniels, 2009). The strong decrease in amplitudes with increasing depth of reflections is mainly controlled by attenuation of the energies of the electromagnetic waves due to conductive electrical properties of the different sediments. Penetration depth in the Rhine gravel depends on electrical properties of different lithofacies, which are mainly dependent on clay content and chemical composition of the pore water. For gravel it varies from a few meters to >20 m for areas with very low apparent electrical conductivities.

GPR measurements are commonly conducted along a surface line to obtain a vertical 2D cross-section of shallow underground structures. Multiple closely-spaced GPR profiles can be combined into a 3D representation (e.g. Beres et al., 1995). Such structural

information has to be supported with borehole or outcrop measurements to correlate the litho-, hydrofacies and/or architectural elements to the reflections. Typically, reflection amplitudes can be correlated to the contrasts between different hydrofacies types. They can be used to identify bounding surfaces and the geometry of internal structures such as foresets of different lithologic zones and bodies. However, no unambiguous evidence of single strata properties can be defined (Heinz and Aigner, 2003a). Hence, GPR profiles are ideally explained by comparison to a well-defined set of default reflection patterns and their associated interpretation. Such radar facies types are not unique and have to be defined for different depositional environments.

Asprion and Aigner (1997, 1999) have examined in detail the characteristic reflection patterns in fluvio-glacial sediments as can be found in the Rhine valley. In line with their work, the GPR profiles obtained for the Herten site will be examined with respect to specific patterns that can be correlated to typical geometric structures, genetic units or architectural elements as identified in the outcrop sections. Accordingly, the measurement and signal filtering procedures as given by Asprion and Aigner (1997) were adopted, and a GSSI (Geophysical Survey Systems Inc., North Salem, NK, USA) radar system (model SIR 10A) with a pair of 300 MHz antenna was applied. Separation of transmitter and receiver was held constant at 1.4 m. Asprion and Aigner (1999) provide a complete description of the field measurement procedure. In a related study, Kowalsky et al. (2001) selected one section of the Herten case study to construct models with various water saturation distributions for GPR forward modeling.

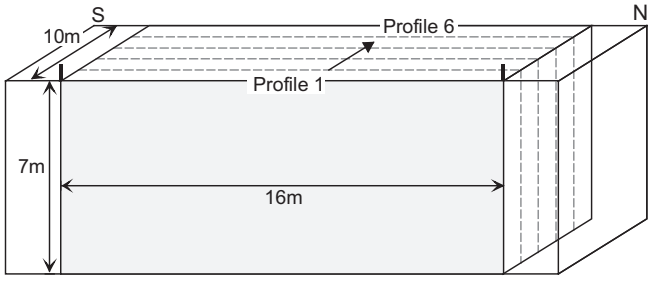

Fig. 3. Orientation of profiles through gravel body (uniform distance between profiles of 2 m). During excavation, a pair of pillars on top was used to mark the position of each new section.

3. Mapping procedure

For the purpose of this mapping, a 16 m × 7 m × 10 m gravel body excavated in the summer of 1999 in the Herten gravel pit was chosen. To reduce the strong attenuation of the GPR-signal, the top-soil containing electrically high loss material has been removed. Then, perpendicular to the desired direction of excavation, parallel GPR measurements were conducted. Finally, unconsolidated sediment until a depth of ca. 9 m was dug out. The excavation extended laterally and did not reach the groundwater table. During the ongoing mining it was possible to obtain a three-dimensional image of the gravel body within a short period of time. The sedimentary body was documented by parallel and equidistant (2 m) vertical sections, which follow the gradual excavation (Fig. 3). From the geophysical measurements, GPR maps could be assigned to each of the cross sections.

Sketches of geological structures were drawn, and small- and large-scale digital photographs were taken from all six cross-sections in order to fully capture 2D heterogeneity on the cm to dm-level. Wide-angle photographs (6 cm × 17 cm, Linhof Technorama 617 S camera with tripod and Schneider centre filter) of the entire outcrop width were scanned and served as basemaps for the digitization procedure. Bedding surfaces and facies boundaries could then be traced to produce digital maps (GIS shape

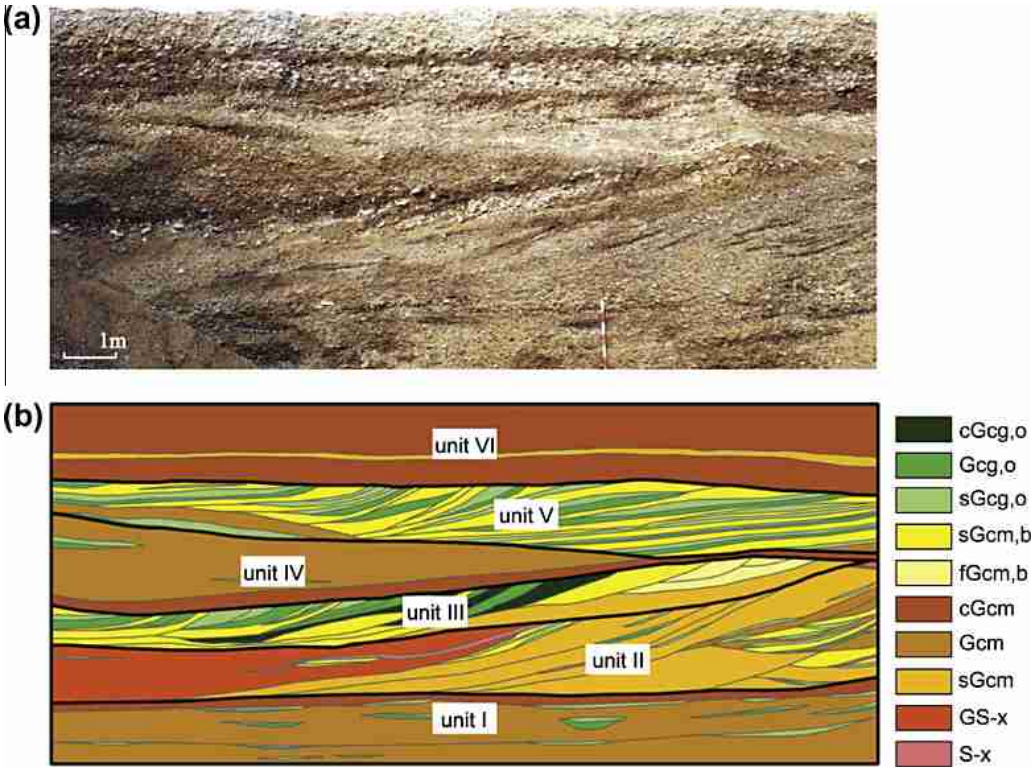

Fig. 4. Profile 4 – (a) outcrop photograph, (b) litho and hydrofacies distribution after digitization with distinction of main genetic units I–VI.

format) that accurately depict the facies distribution on each face. As a result, six parallel portrayals of litho-, hydro- and radar facies were obtained. In this manner, the basis for the production of an interpolated full 3D-model was created (Maji, 2005; Comunian et al., 2011).

As an example, Fig. 4 depicts inner Section 4. Even with the low resolution outcrop photo shown here (Fig. 4a), major structures can be delineated. This is due to the variability of material, water content and excavation stability specific to different facies types. Furthermore, in matrix-rich compartments, drying of the exposure wall surface from the sunny weather was less effective, a fact that increased the visual contrasts.

4. Results

4.1. Architectural elements

The digitization procedure and facies-based distinction delivered six very similar facies mosaics for each of the vertical profiles

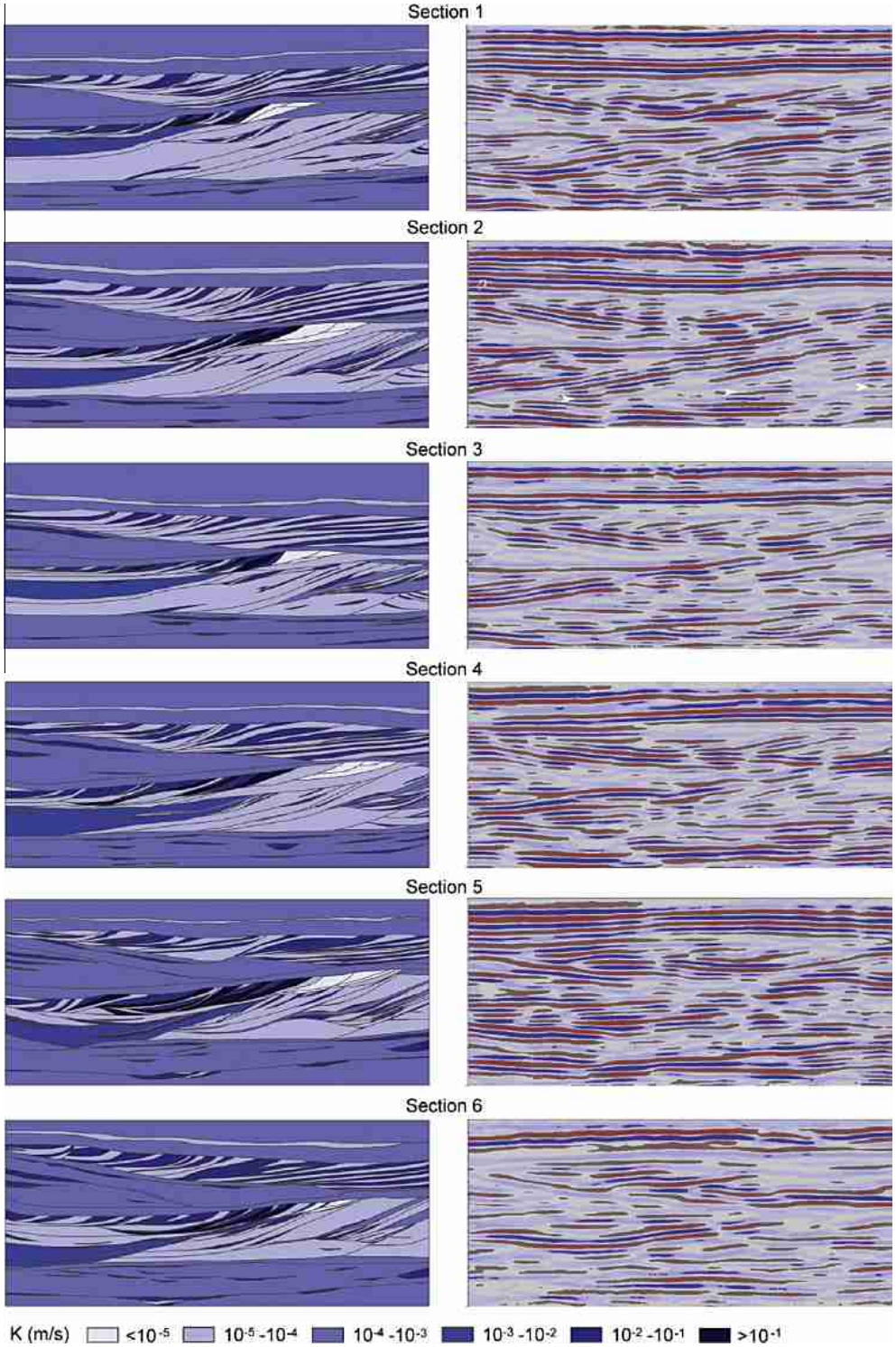

Fig. 5. Hydrofacies based conductivity map (left) and corresponding GPR profiles of Sections 1–6.

(Fig. 5, Nos. 1–6 in the direction of excavation) with typical, recurring patterns. In all sections, we can distinguish six major genetic units that are dominated by specific architectural elements. These units can be distinguished, from bottom to top, as follows (Fig. 4b):

Unit I: The lowermost unit consists of sand-rich, poorly sorted gravel intercalated with patches and discontinuous beds of openwork gravels (10–20 cm in thickness) which indicate subhorizontal stratification.

Unit II: A heterogeneous thick unit with local small sections through alternating sequences, with variably cross-bedded poorly sorted gravel dipping to the South and a massive well sorted gravel body in the Southern (left) half.

Unit III: A trough-shaped, relatively thin and continuous unit with mainly alternating sequences, dipping in a Southern direction.

Unit IV: A wedge-shaped sand-rich, poorly sorted gravel deposit with discontinuous thin beds of openwork gravels that indicate cross stratification gently dipping to the North.

Unit V: A laterally extended unit with heterogeneous sequences of inclined, concave and trough-shaped bimodal gravel and open frameworks; dipping to the South, similar to unit III.

Unit IV: Horizontally stratified, thick continuous gravel sheets in the uppermost ca. 1.5 m of the outcrop.

The geometry of the bounding surfaces and the dip of the tangential and parallel foresets are indicators that the sections are oriented almost parallel to the mean ancient flow direction. Genetic units III and V can be interpreted as typical scour pool fillings that originate from pools moving to the South with sedimentation of alternating sequences downstream. The bimodal couples found in the units II, III and V portray the existence of flow separation zone developing at the transition from the channel into the scour. These scour pool fillings represent architectural elements with erosion as well as deposition character. The size of lower unit III slightly increases in direction of excavation with greatest extension in profiles 5 and 6. This could also indicate a trough shape in this direction. Unit IV represents a gravel sheet, which is genetically related to the scours (e.g. Marti, 2002). Alternating sequences sporadically appear also in unit V. These can be interpreted as partly eroded relics of former more extensive scour pool fills. Particularly in the Northern part, a wedge-shaped zone in the cross section can be found in all profiles that could be the beginning of a further big scale scour pool fill that dominates beyond the mapping boundaries. While the rather homogeneous units I and V cannot be easily categorized, unit VI shows typical features of erosive gravel sheets. Such gravel sheets are typical architectural elements, in particular in the more distant glacier outwash area. Therefore, its appearance on top of the profiles could indicate a later phase of outwash deposition during further retreat of the glacier. The transition between units V and VI is also described at different localities in NE-Switzerland, e.g. Hüntwangen pit (Siegenthaler and Huggenberger, 1993).

4.2. Litho- and hydrofacies distribution

The hydrofacies show the highest variation in the alternating sequences (lithofacies *Gcg, a*) that dominate units III and V. These alternating sequences account for about 25% of the profiles. The sandy bimodal gravel (*sGcg,b*) clearly dominates the base of the sequences. The finer *fGcg,b* common to *Gcg,a* sequences only appears rarely and concentrated locally as trough-shaped deposits in the Northern part of unit III (in profiles 1–5). The highly permeable coarse framework gravels (*cGcg, o*) also occur exclusively in this central unit. They are most pronounced in profile 5. The total portion of open framework is about 10% on the average and slightly increases towards the (Western) direction of excavation (Fig. 6).

The preeminent lithofacies (ca. 70%) is the matrix-supported gravel (*Gcm*) with the hydrofacies variants *sGcm*, *cGcm*, *Gcm*. In contrast to the alternating sequences, they commonly show larger

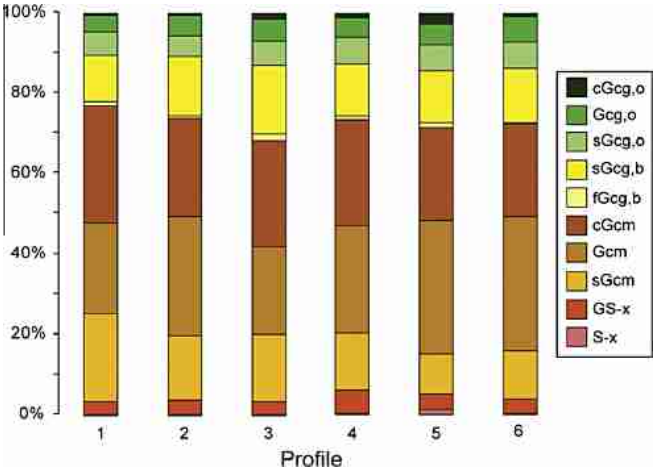

Fig. 6. Areal percentage of hydrofacies classes in the six profiles.

extensions and more continuity from one section to the next. For example, top unit VI is built up by a continuous *cGcm – sGcm – cGcm* strata in all profiles. Such continuous *cGcm* gravel sheets also represent the top of unit I and the basis of unit IV. Compared with the homogeneous unit VI, the matrix-supported gravel in the other units is frequently interbedded by local trough-shaped or thin-layered framework.

Unit II is dominated by the sandy matrix-supported gravel. Therefore, as depicted in the log-based conductivity profiles (Fig. 5), it is an extensive zone of low conductivity. Only in this unit, a substantial *GS-x* wedge can be found which increases its size towards the direction of excavation. It represents a continuous zone of relatively high conductivity. Overall, well sorted lithofacies *GS-x* and *S-x* are rare, and the latter represents less than 1% in the profiles.

4.3. Radar profiles

Fig. 5 compares the derived conductivity maps to the GPR profiles, and shows that several typical structures and bedforms are well captured by GPR. Radar permittivity and reflection is controlled especially by the residual water content contrasts. Thus hydrofacies boundaries are ideally reproduced if they are significant and continuous such as at the interfaces between some genetic units and within alternating sequences. This is true in particular between and within the upper units. The horizontal layering of the homogeneous gravel sheet that makes up top unit VI can be directly correlated from the outcrop facies maps to the continuous horizontal high-amplitude reflectors in the upper part of the radar profiles (see top arrow GPR profile of Section 3). The following lower unit V is separated clearly from unit VI by commonly short, dipping reflectors that delineate the internal cross-beddings of the bundles of alternating gravel. Interestingly, the amplitudes of these reflections increase towards the bottom, which could reflect drainage in the upper part and ponding of residual water in the lower. A basal strong reflection of unit V originates from the contrast to the underlying massive matrix-supported gravel of unit IV.

The alternating sequences generate considerable small-scale contrasts, apparently delineating the substantial hydraulic contrasts between clast-supported and matrix-supported facies types. Especially on the Southern part, reflection dips of unit V follow the relatively horizontal layering, whereas the inclined reflections of the Northern part indicate the cross-beddings and more concave, inclined alternating sequences. Nevertheless, resolution is limited, and even though the radar profiles reproduce characteristic

features well, individual beds are rarely resolved. Overall, the reflectors help to reconstruct the sequences, although the reflection volume limits depiction of small scale features. Radar facies determined based on these GPR maps thus would have to be based on the genetic units rather than single facies variability.

Deeper units are more difficult to correlate with the GPR profiles. While the wedge-shaped form of unit IV can be identified also in the reflections, it is hardly possible to deduce from radar information alone that it is underlain by a thin high-conductivity unit V. This is certainly due to the resolution that technically decreases with the profile depth, and due the small width of unit III that cannot be resolved by the given wavelength. Again, internal lithofacies variations can hardly be interpreted by the radar profiles alone. As an exception, the major structural trends in the basal units, cross-beddings and trough-shaped bedforms in unit II and more horizontal layers in unit I, can be seen in the reflector patterns. This enables the tracing of the boundary between the units in the radar profiles, where inclined reflectors downlap on basal horizontal reflectors (as accentuated by the arrows on the GPR profile for Section 2, Fig. 5).

5. Conclusions

A high resolution portrayal of a braided river deposit block was developed, which is considered one of the best characterized gravel bodies of this size. Combination of sedimentary and hydrogeological facies analysis enabled a reliable structural analysis on decimeter and meter scale. The gravel body was investigated by recording full 2D cross sections during excavation. The sections were digitized based on outcrop drawings and photographs. Facies mosaics are attained, for each of which a sequence of six characteristic genetic sedimentary units can be distinguished. The facies mosaics were compared to GPR profiles. The latter had been obtained from a survey before the excavation. In particular the best resolved upper part of the profiles delivers characteristic reflection patterns. Continuous high amplitudes correlate with layered gravel sheets and inclined small-scale reflections delineate alternating gravel sequences as deposited in scour pools. These patterns would be suitable for framing radar facies types. For the lower units in the gravel body, interpretation of the GPR profiles would be ambiguous without the facies maps.

The gravel body is highly heterogeneous, in particular in the alternating sequences of units III and V, and at other parts where highly conductive open frameworks are embedded in matrix supported gravel beds. Continuity in the third dimension, towards the direction of excavation, can be assessed by sequential comparison of neighboring facies profiles. It is revealed that the major genetic units recur in each section, with slight variability and some trends in the unit boundaries. Among the individual hydrofacies zones, only larger layers and wedges show continuity. Those with high variability in the 2D section such as again the alternating sequences cannot easily be traced in the third dimension.

This presentation is intended to offer more insight into the underlying "real time" mapping procedure as well as into the types of sedimentological, hydrogeological and geophysical data available. It is also meant to stimulate further use of the presented data in future applications. Of particular interest are analog simulations of flow and transport processes. Results from such simulations can be interpreted for similar but incompletely described aquifers, or for hardly accessible deep aquifers with similar facies distribution. For example, the role of sedimentary heterogeneity on dispersive processes relevant for successful carbon dioxide sequestration in comparable sediments can be examined. Also, the detailed resolution of the structures facilitates numerical simulations to study non-Fickian transport behavior. The data set, in 2D sections or reconstructed in 3D, is certainly perfect grounds for testing and validating innovative hydrogeological modeling concepts. The efficiency of both forward and inverse modeling techniques can be demonstrated on a highly realistic and fully digitalized field case.

Acknowledgements

This work was supported by the German Research Foundation (DFG) and the Swiss National Science Foundation (SNF) Sinergia Project "Ensemble". The diligent assistance of Margaret Hass during the preparation of the manuscript is highly acknowledged. Special thanks go to Jürgen Heinz, Georg Teutsch, Thomas Aigner and Gerhard Lörcher for their support during mapping, digitization and facies interpretation at the University of Tübingen. Semere Solomon and two anonymous reviewers substantially helped to improve the original version of the manuscript.

Appendix A. Supplementary material

Supplementary data associated with this article can be found, in the online version, at doi:10.1016/j.jhydrol.2011.03.038.

References

Anderson, M.P., 1989. Hydrogeologic facies models to delineate large-scale spatial trends in glacial and glaciofluvial sediments. Geol. Soc. Am. Bull. 101 (4), 501–511.

Anderson, M.P., Aiken, J.S., Webb, E.K., Mickelson, D.M., 1999. Sedimentology and hydrogeology of two braided stream deposits. Sediment. Geol. 129 (3–4), 187–199.

Asprion, U., Aigner, T., 1997. Aquifer architecture analysis using ground penetrating radar: triassic and quaternary examples (S Germany). Environ. Geol. 28, 1–10.

Asprion, U., Aigner, T., 1999. Towards realistic aquifer models: a three-dimensional georadar case study of quaternary gravel deltas (Singen Basin, SW Germany). Sediment. Geol. 129 (3–4), 281–297.

Bayer, P., 2000 Aquifer-Analog-Studie in grobklastischen 'braided river' Ablagerungen: sedimentäre/hydrogeologische Wandkartierung und Kalibrierung von Georadarmessungen – Diplomkartierung. University of Tübingen, unpublished.

Becht, A., Bürger, C., Kostic, B., Appel, E., Dietrich, P., 2007. High-resolution aquifer characterization using seismic cross-hole tomography: an evaluation experiment in a gravel delta. J. Hydrol. 336 (1–2), 171–185.

Beres, M., Green, A.G., Huggenberger, P., Horstmeyer, H., 1995. Detailed 3-D georadar studies of glaciofluvial sediments. Geology 12, 1087–1091.

Bersezio, R., Giudici, M., Mele, M., 2007. Combining sedimentological and geophysical data for high-resolution 3-D mapping of fluvial architectural elements in the quaternary Po plain. Sediment. Geol. 202 (1–2), 230–248.

Brauchler, R., Hu, R., Vogt, T., Halbouni, D., Heinrichs, T., Ptak, T., Sauter, M., 2010. Cross-well slug interference tests: An effective characterization method for resolving aquifer heterogeneity. J. Hydrol. 384 (1–2), 33–45.

Chen, J., Rubin, Y., 2003. An effective Bayesian model for lithofacies estimation using geophysical data. Water Resour. Res. 39 (5), 1118. doi:10.1029/2002WR001666.

Chen, X., Song, J., Wang, W., 2010. Spatial variability of specific yield and vertical hydraulic conductivity in a highly permeable alluvial aquifer. J. Hydrol. 388 (3–4), 379–388.

Comunian, A., Straubhaar, J., Bayer, P., Renard, P., 2011. Three-dimensional high resolution fluvio-glacial aquifer analog: Part 2: geostatistical modelling. J. Hydrol. 405 (1–2), 10–23.

Dafflon, B., Irving, J., Holliger, K., 2010. Calibration of high-resolution geophysical data with tracer test measurements to improve hydrological predictions. Adv. Water Resour. 33 (1), 55–68.

Daniels, D.J., 2009. Antennas. In: Jol, H.M. (Ed.), Ground Penetrating Radar: Theory and Applications. pp. 104–139.

Ezzy, T., Cox, M., O'Rourke, A., Huftile, G., 2006. Groundwater flow modelling within a coastal alluvial plain setting using a high resolution hydrofacies approach. Hydrogeol J. 14 (5), 675–688.

Fraser, G.S., Davis, J.M., 1998. Hydrogeologic Models of Sedimentary Aquifers, SEPM Concepts in Hydrogeology and Environmental Geology, vol. 1. Soc. for Sediment. Geol, Tulsa, OK. 180 pp..

Heinz, J., Aigner, T., 2003a. Three-dimensional GPR analysis of various quaternary gravel-bed braided river deposits (southwestern Germany). In: Bristow, C.S., Jol, H.M. (Eds.), Ground Penetrating Radar in Sediments, vol. 211. Spec. Publ. Geol. Soc., London, pp. 99–110.

Heinz, J., Aigner, T., 2003b. Hierarchical dynamic stratigraphy in various quaternary gravel deposits, Rhine glacier area (SW Germany): implications for hydrostratigraphy. Int. J. Earth Sci. 92, 923–938.

Heinz, J., Kleineidam, S., Teutsch, G., Aigner, T., 2003. Heterogeneity patterns of quaternary glaciofluvial gravel bodies (SW-Germany): application to hydrogeology. Sediment. Geol. 158 (1–2), 1–23.

Hu, R., Brauchler, R., Herold, M., Bayer, P., Sauter, M., 2009. A hydraulic tomography approach coupling travel time inversion with steady shape analysis based on aquifer analogue study in coarsely clastic fluvial glacial deposits. EGU General Assembly, Vienna.

Huggenberger, P., Siegenthaler, C., Stauffer, F., 1988. Grundwasserströmung in Schottern; Einfluss von Ablagerungsformen auf die Verteilung der Grundwasserfliessgeschwindigkeit. Wasserwirtschaft 78 (5), 202–212.

Huggenberger, P., 1993. Radar facies: recognition of facies patterns and heterogeneities within Pleistocene Rhine gravels, NE Switzerland. In: Best, J.L., Bristow, C.S. (Eds.), Braided Rivers, vol. 75. Spec. Publ., Geol. Soc. London, pp. 163–176.

Huggenberger, P., Aigner, T., 1999. Introduction to the special issue an Aquifer-sedimentology: problems, perspectives and modern approaches. Sediment. Geol. 129 (3–4), 179–186.

Huysmans, M., Peeters, L., Moermans, G., Dassargues, A., 2008. Relating small-scale sedimentary structures and permeability in a cross-bedded aquifer. J. Hydrol. 361 (1–2), 41–51.

Hyndman, D., Tronicke, J., 2005. Hydrogeophysical studies at the local scale: the saturated zone. In: Hydrogeophysics, vol 50. Water Science and Technology Library, Springer, NY. pp. 391–412.

Iversen, B.V., van der Keur, P., Vosgerau, H., 2008. Hydrogeological relationships of sandy deposits: modeling of two-dimensional unsaturated water and pesticide transport. 37(5), 1909–1917.

Jol, H.M., 2009. Ground penetrating radar: theory and applications. Elsevier Ltd.. 544 p..

Jussel, P., Stauffer, F., Dracos, T., 1994. Transport modeling in heterogeneous aquifers, 1. Statistical description and numerical generation of gravel deposits. Water Resour. Res. 30 (6), 1803–1817.

Keller, B., 1996. Lithofazies-Codes für die Klassifikation von Lockergesteinen. Mitt. Schweiz. Gesell. Boden Felsmechanik 132, 5–12.

Kleineidam, S., 1998. Der Einfluss von Sedimentologie und Sedimentpetrographie auf den Transport gelöster organischer Schadstoffe im Grundwasser [Impact of sedimentology and sedimdent petrography on the fate and transport of organic compounds in groundwater]. PhD Thesis, Tübinger Geowissenschaftliche Arbeiten, 41, Germany.

Kleineidam, S., Rügner, H., Grathwohl, P., 1999. Influence of petrographic composition/organic matter distribution of fluvial aquifer sediments on the sorption of hydrophobic contaminants. Sediment. Geol. 129 (3–4), 311–325.

Klingbeil, R., Kleineidam, S., Asprion, U., Aigner, T., Teutsch, G., 1999. Relating lithofacies to hydrofacies: outcrop-based hydrogeological characterisation of quaternary gravel deposits. Sediment. Geol. 129 (3–4), 299–310.

Kock, S., Huggenberger, P., Preusser, F., Rentzel, P., Wetzel, A., 2009. Formation and evolution of the lower Terrace of the Rhine River in the area of Basel, Swiss. J. Geosci. 102, 307–321.

Kostic, B., Becht, A., Aigner, T., 2005. 3-D sedimentary architecture of a quaternary gravel delta (SW Germany): implications for hydrostratigraphy. Sediment. Geol. 181 (3–4), 143–171.

Kowalsky, M.B., Dietrich, P., Teutsch, G., Rubin, Y., 2001. Forward modeling of ground-penetrating radar data using digitized outcrop images and multiple scenarios of water saturation. Water Resour. Res. 37 (6), 1615–1625.

Maier, U., Becht, A., Kostic, B., Bürger, C., Bayer, P., Teutsch, G., Dietrich, P., 2005. Characterization of quaternary gravel aquifers and their implementation in hydrogeological models. In: Proceedings of GQ2004. 4th International Groundwater Quality Conference, vol. 297 Waterloo, Canada, July 2004, IAHS Publ, pp. 159–168.

Maier, U., DeBiase, C., Baeder-Bederski, O., Bayer, P., 2009. Calibration of hydraulic parameters for large-scale vertical flow constructed wetlands. J. Hydrol., doi: 10.1016/j.jhydrol.2009.02.032.

Maji, R., 2005. Conditional stochastic modelling of DNAPL migration and dissolution in a high-resolution aquifer analog. PhD Thesis, Dept of Earth Sciences, University of Waterloo.

Maji, R., Sudicky, E.A., Panday, S., Teutsch, G., 2006. Transition probability/Markov chain analysis of DNAPL source-zones and plumes. Ground Water 44 (6), 853–863. doi:10.1111/j.1745-6584.2005.00194.x.

Marti, C., 2002. Morphodynamics of widenings in steep rivers. In: Bousmar, D., Zech, Y., (Eds.), River Flow, vol. 2. pp. 865–873.

Ouellon, T., Lefebvre, R., Marcotte, D., Boutin, A., Blais, V., Parent, M., 2008. Hydraulic conductivity heterogeneity of a local deltaic aquifer system from the kriged 3D distribution of hydrofacies from borehole logs, Valcartier. Can. J. Hydrol. 351, 71–86.

Scheibe, T., Freyberg, D.L., 1995. The use of sedimentological information for geometric simulation of natural porous media structure. Water Resour. Res., 3259–3270.

Siegenthaler, C., Huggenberger, P., 1993. Pleistocene Rhine gravel: deposits of a braided river system with dominant pool preservation. In: Best J.L., Bristow C.S. (Eds.), Braided Rivers. Geological Society, (special publication 75), pp. 147–162.

Smith, S.A., 1989. Sedimentation in a meandering gravel-bed river: the River Tywi, South Wales. Geol J. 24, 193–204.

Stanford, S.D., Ashley, G.M., 1998. Using three-dimensional geologic models to map glacial aquifer systems: an example from New Jersey. In: Fraser, G.S., Davis, J.M. (Eds.), Hydrogeologic Models of Sedimentary Aquifers: Concepts in Hydrogeology and Environmental Geology, no 1 SEPM, vol 1. Oklahoma, USA, pp. 69–84.

Weissmann, G.S., Fogg, G.E., 1999. Multi-scale alluvial fan heterogeneity modeled with transition probability geostatistics in a sequence stratigraphic framework. J. Hydrol. 226 (1–2), 48–65.

Werth, C.J., Cirpka, O.A., Grathwohl, P., 2006. Enhanced mixing and reaction through flow focusing in heterogeneous porous media. Water Resour. Res. 42, W12414.

Zappa, G., Bersezio, R., Felletti, F., Giudici, M., 2006. Modeling heterogeneity of gravelsand, braided stream, alluvial aquifers at the facies scale. J. Hydrol. 325, 134–153.